

Surviving rapid climate change in the deep sea during the Paleogene hyperthermals

Laura C. Foster^{a,1}, Daniela N. Schmidt^a, Ellen Thomas^{b,c}, Sandra Arndt^d, and Andy Ridgwell^d

^aDepartment of Earth Sciences, University of Bristol, Bristol BS8 1RJ, United Kingdom; ^bDepartment of Geology and Geophysics, Yale University, New Haven, CT 06520; ^cDepartment of Earth and Environmental Sciences, Wesleyan University, Middletown, CT 06459; and ^dSchool of Geographical Sciences, University of Bristol, Bristol BS8 1SS, United Kingdom

Edited* by Karl K. Turekian, Yale University, New Haven, CT, and approved April 23, 2013 (received for review January 14, 2013)

Predicting the impact of ongoing anthropogenic CO₂ emissions on calcifying marine organisms is complex, owing to the synergy between direct changes (acidification) and indirect changes through climate change (e.g., warming, changes in ocean circulation, and deoxygenation). Laboratory experiments, particularly on longer-lived organisms, tend to be too short to reveal the potential of organisms to acclimatize, adapt, or evolve and usually do not incorporate multiple stressors. We studied two examples of rapid carbon release in the geological record, Eocene Thermal Maximum 2 (~53.2 Ma) and the Paleocene Eocene Thermal Maximum (PETM, ~55.5 Ma), the best analogs over the last 65 Ma for future ocean acidification related to high atmospheric CO₂ levels. We use benthic foraminifers, which suffered severe extinction during the PETM, as a model group. Using synchrotron radiation X-ray tomographic microscopy, we reconstruct the calcification response of survivor species and find, contrary to expectations, that calcification significantly increased during the PETM. In contrast, there was no significant response to the smaller Eocene Thermal Maximum 2, which was associated with a minor change in diversity only. These observations suggest that there is a response threshold for extinction and calcification response, while highlighting the utility of the geological record in helping constrain the sensitivity of biotic response to environmental change.

marine calcifiers | greenhouse gases | ecosystem stress response

Since the industrial revolution, approximately one-third of carbon dioxide (CO₂) released in the atmosphere has been absorbed by the oceans, which has resulted in a lowering of seawater carbonate saturation and a reduction of the average surface pH by 0.1 pH unit, with further reduction by 0.14–0.35 pH units predicted toward the end of the 21st century (1). Such changes in seawater chemistry are predicted to significantly affect marine calcifiers. Culturing experiments, however, have documented a complex range of responses, including dissolution of carbonate shells/skeletons, slower growth, reproductive failure, and reduced activity (1), which makes specific predictions difficult. Evaluating the potential impact of ocean acidification on whole ecosystems is even more complicated, because acidification acts synergistically with other stressors such as global warming and deoxygenation, and competitive advantage/disadvantage is difficult to forecast. In addition, ocean acidification occurs progressively and on a century time scale—much longer than can be replicated in the laboratory. Experiments, particularly on longer-lived organisms, hence tend to be too short to detect the potential for organisms to acclimatize, adapt, or evolve in response to changing environments and cannot predict which traits are most useful. In contrast, the geological record of rapid carbon release may function as an analog for our next century and allows us to examine long-term adaptive strategies of organisms to multiple stressors.

During the hyperthermals of the Paleocene and Eocene (65.5–33.7 Ma), isotopically light carbon was rapidly released into the ocean–atmosphere system, leading to global warming and deep-sea carbonate dissolution (2). The most prominent of these, the Paleocene Eocene Thermal Maximum (PETM, ~55.5 Ma), has

been cited as one of the best analogs for the future (3), although such events are likely to represent only minimum estimates of future biotic and ecosystem changes because the rate of change in surface saturation during the PETM probably was an order of magnitude lower than the present and future rate (4). The release of isotopically light carbon during the PETM resulted in rapid (<10,000 y) global warming with a maximum temperature increase of the surface ocean locally as large as 9–10 °C and of the deep sea 4–5 °C (5–9). The warming led to migration of low-latitude species toward higher latitudes and fast evolutionary turnover (10, 11). The carbon input caused a global negative Carbon Isotope Excursion (CIE) of >2.5‰ (6) and lowered ocean pH and carbonate ion concentration ([CO₃²⁻]), resulting in a rapid shoaling of the Calcite Compensation Depth (CCD) (2). Associated with this global perturbation were a range of biotic changes, most prominently in deep-sea benthic foraminifera, which experienced their only significant global extinction (35–50%) in the last 90 million years (9). Marine calcifying plankton (foraminifera and calcareous nannoplankton), in contrast, did not suffer severe extinction, despite the rapid, in part transient, evolutionary turnover, and carbonate production by nannoplankton may not have been significantly affected (12).

Eocene Thermal Maximum 2 (ETM-2, ~53.2 Ma) occurred about 2 million years after the PETM and provides the opportunity for a comparative study, because it is qualitatively similar to the PETM, with only about half its magnitude (13). Benthic foraminiferal assemblages declined in diversity with postexcursion assemblages similar to the low-diversity post-PETM ones (13–15), but without significant extinction. Carbonate dissolution occurred and the lysocline rose, but the CCD did not shoal to (or beyond) the depth of the sites in the southeast Atlantic where dissolution was complete during the PETM (16). The geological record thus provides an ideal opportunity to assess the sensitivity of marine organisms to contrasting magnitudes of global warming, ocean acidification, and related stressors, thereby assessing potential future thresholds for adaptation and acclimatization.

To examine the response of benthic foraminifera to hyperthermal environmental changes, we selected samples from Ocean Drilling Program (ODP) sites 1262 (27°11.15'S, 1°34'2'E) and 1263 (28°31.98'S, 2°46.77'E) on Walvis Ridge (southeastern Atlantic Ocean), paleodepths 3.5 and 1.5 km, respectively. We combined assemblage analysis with synchrotron radiation X-ray tomographic microscopy (SRXTM) at the Tomographic Microscopy and Coherent Radiology Experiments (TOMCAT) beamline at the Swiss Light source, Paul Scherrer Institute to generate high-resolution (0.37 μm), 3D images of specimens of two deep-sea benthic

Author contributions: L.C.F., D.N.S., E.T., and A.R. designed research; L.C.F. and D.N.S. performed research; L.C.F., D.N.S., and S.A. contributed new reagents/analytic tools; L.C.F. and D.N.S. analyzed data; and L.C.F., D.N.S., E.T., and A.R. wrote the paper.

The authors declare no conflict of interest.

*This Direct Submission article had a prearranged editor.

¹To whom correspondence should be addressed. E-mail: l.c.foster@bristol.ac.uk.

This article contains supporting information online at www.pnas.org/lookup/suppl/doi:10.1073/pnas.1300579110/-DCSupplemental.

foraminiferal species that survived the PETM: the extant, shallow-infaunal *Oridorsalis umbonatus* and the extinct, probably epifaunal *Nuttallides truempyi*. A total of 61 specimens were analyzed. We quantified their test volumes, number of chambers (proxy for life span), number and volume of pores, size of their first chamber (proxy for reproductive mode), and the amount of calcite precipitated with unequalled precision. Studies of calcification of planktic foraminifera during glacial–interglacial times (and by inference, their test wall thickness) led us to expect a significant decrease in calcite precipitated at the lower saturation states during the PETM (17). Our data provide a unique insight into the response of deep-sea calcifiers to past episodes with strong similarities to the potential future consequences of fossil fuel CO₂ emissions (1–3).

Results

At the onset of the PETM CIE, about 35% of benthic foraminiferal taxa became extinct, and rarefied benthic foraminiferal diversity declined from an average of ~55 to ~20, with minimum values of 15 (Fig. 1). Postextinction assemblages were strongly dominated by a few species, including *Nuttallides truempyi*, *Oridorsalis umbonatus*, and various abyssaminid species.

Individual specimens of *O. umbonatus* that were calcifying shortly after the onset of the PETM at ODP site 1263 (~13.5 thousand years after the event initiation, the earliest sediment where calcite is again present), against our expectation, have thicker walls relative to test diameter than those calcifying before and after the PETM (Fig. 1, Table 1, and [Datasets S1](#) and [S2](#); $P < 0.05$, ANOVA). Increased calcification continued after the end of the CIE, as indicated by significant differences in the volume of normalized calcite deposited before, during, and after the PETM ($P < 0.05$, ANOVA). Specimens from the deeper ODP site 1262, which has a thicker carbonate-free sediment zone (corresponding to a longer time) (18) without foraminifers, show a similar response, but the more severe dissolution makes precise quantification of its extent difficult.

The epifaunal *N. truempyi* was absent from the sediment for a longer time after the onset of the PETM than the infaunal *O. umbonatus* but shows the same response, that is, it also has

Table 1. Summarized calcification data for ODP site 1263

| Age since CIE, thousands of years | Penultimate chamber width/maximum test width, % | Volume of normalized calcite, % |
|-------------------------------------|-------------------------------------------------|---------------------------------|
| Site 1263 PETM <i>O. umbonatus</i> | | |
| 160.3 | 3.7 | 52.5 |
| 144.4 | 2.5 | 64.0 |
| 124.7 | 3.6 | 55.1 |
| 115.7 | 4.2 | 57.5 |
| 107.5 | 3.0 | 65.3 |
| 107.5 | 3.4 | 60.6 |
| 101.9 | 4.1 | 65.3 |
| 57.6 | 2.0 | 63.9 |
| 39.8 | 6.9 | 64.5 |
| 27.8 | 6.6 | 69.2 |
| 27.8 | 5.8 | 71.4 |
| 27.8 | 6.1 | 74.8 |
| 27.8 | 6.9 | 65.2 |
| 27.8 | 5.4 | 66.2 |
| 13.5 | 5.5 | 75.4 |
| -79.9 | 2.2 | 51.6 |
| -127.4 | 1.7 | 55.4 |
| -127.4 | 4.4 | 46.1 |
| -127.4 | 2.5 | 54.0 |
| -127.4 | 2.8 | 56.3 |
| -127.4 | 4.2 | 56.3 |
| -127.4 | 2.7 | 55.8 |
| Site 1263 PETM <i>N. truempyi</i> | | |
| 159.4 | 1.6 | 41.1 |
| 103.4 | 2.2 | 55.1 |
| 57.6 | 2.3 | 62.8 |
| 39.8 | 4.3 | 59.4 |
| -79.9 | 3.0 | 54.1 |
| -127.4 | 2.1 | 58.6 |
| Site 1263 ETM-2 <i>O. umbonatus</i> | | |
| 93.1 | 2.7 | 64.4 |
| 67.7 | 3.7 | 54.6 |
| 53.8 | 2.5 | 58.7 |
| 38.7 | 2.2 | 54.7 |
| 37.8 | 6.9 | 60.4 |
| 36.8 | 3.5 | 58.8 |
| 35.8 | 4.3 | 63.3 |
| 30.5 | 2.8 | 48.7 |
| 13.2 | 4.3 | 69.0 |
| -2.7 | 5.1 | 63.2 |

Data show the maximum relative width of the penultimate chamber and amount of calcite preserved (size normalized) for the PETM for *O. umbonatus*, *N. truempyi*, and for ETM-2 *O. umbonatus* only (full data are provided in [Dataset S1](#)).

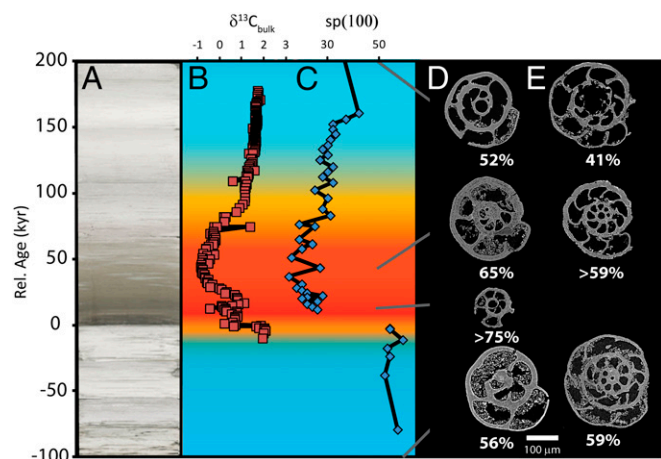


Fig. 1. ODP site 1263 Walvis Ridge (A) digital core image with (B) $\delta^{13}\text{C}$ record (‰) (2) and (C) rarefied number of species [sp(100)] plotted against numerical age from the onset of the PETM in thousands of years (kyr) (38) ([Dataset S3](#)), (D) with tomographic reconstruction of cross-sections of *O. umbonatus* and (E) *N. truempyi*. The amount of calcite preserved is given relative to the test volume to correct for size effects. The color indicates temperature variation during the PETM, with temperature increasing from blue (cooler) to red (warmer) temperatures (18). The color of the sediments reflect CaCO₃ content, with darker colors indicating lower CaCO₃.

thicker walls (approximately doubling in thickness) relative to test diameter. The severity of the dissolution combined with the greater fragility of its test due to the numerous large pores made it impossible to analyze a complete specimen to determine the volume of calcium carbonate. The incomplete specimen of *N. truempyi* from the PETM of site 1263, however, had the same volume of calcium carbonate as the specimen from below the CIE, so that its volume, if complete, would have exceeded the preevent value. At the deeper site 1262, the oldest post-PETM specimen that could be analyzed lived ~74.8 thousand years after the onset of the CIE (i.e., well into the recovery), so we cannot assess calcite volume or wall thickness during the peak CIE.

During ETM-2, CaCO₃ dissolution was much less severe (16). The foraminiferal diversity had not fully recovered after the PETM extinction about 2 million years earlier, with average rarefied values around 40, declining to about 27 during ETM-2 (Fig. 2). No species

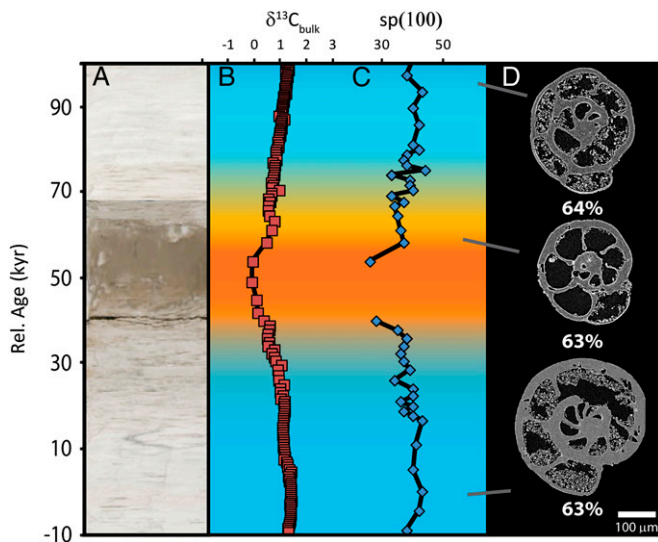


Fig. 2. ODP site 1263 Walvis Ridge (A) digital core image with (B) $\delta^{13}\text{C}$ record (‰) (14) and (C) rarefied number of species [sp(100)] plotted against numerical age from the onset of ETM-2 in thousands of years (kyr) (38) (Dataset S3) (D) with tomographic reconstruction of cross-sections of *O. umbonatus*. The amount of calcite preserved is given relative to the test volume to correct for size effects. The color indicates temperature variation during the ETM-2 with temperature increasing from blue (cooler) to red (warmer) temperatures (14). The color of the sediments reflect CaCO_3 content, with darker colors indicating lower CaCO_3 .

became extinct, but lowest-diversity assemblages were dominated by the same taxa as the post-PETM ones, i.e., *O. umbonatus*, *N. truempyi*, and abyssaminids (16). *O. umbonatus* shows no significant changes in wall thickness or volume-normalized calcite (Fig. 2), with a maximum volume-normalized calcite of up to 69% for ETM-2 compared with 75% during the PETM (Dataset S1).

Discussion

Based on comparison with other foraminiferal studies, and without direct experiments available of the effect of varying pH on deep-sea foraminifers, one would expect that deep-sea benthic foraminifera would decrease calcification in response to acidification. Foraminifera raise their internal pH (19) during calcification, and thus require additional energy to calcify at lower saturation. For instance, planktic foraminifera produced heavier shells during glacial times when the partial pressure of atmospheric CO_2 was lower and $[\text{CO}_3^{2-}]$ higher (17), and thinner tests when cultured under lowered $[\text{CO}_3^{2-}]$ (20). Culture studies of shallow-water benthic species that do not contain photosymbionts show decreased calcification (thinner test walls) at lower pH values (21–23). In contrast, *O. umbonatus* deposited significantly more CaCO_3 normalized to test volume (volume-normalized calcite) during the PETM in sediment showing strong carbonate dissolution. This is unlikely to result from a biased loss of more fragile specimens in these populations due to dissolution, because thick specimens were not found before the CIE. Additionally, detailed investigation of preservation using SRXTM shows a lack of severe dissolution in the thick specimens from site 1263, thereby making selective dissolution as a cause of the pattern unlikely. Increased calcification in *O. umbonatus* occurred in response to the environmental changes associated with the PETM but not during ETM-2, consistent with the existence of a threshold response to the magnitude of environmental perturbation.

The cause of the deep-sea benthic foraminiferal extinction itself during the PETM is not clear (9). Significant deep-sea extinctions are very rare, because the habitat is enormous and benthic foraminifera produce motile stages (propagules) during

sexual as well as asexual reproduction, so that they can rapidly recolonize from refugia. Proposed causes include deoxygenation, decreased food supply, and/or increased metabolic rates (9). The fact that metazoan benthic ostracods, with much more limited dispersal potential than benthic foraminifera (24), did not suffer severe global extinction (e.g., ref. 25) is an argument against deoxygenation as an important cause, because active arthropods are more sensitive to low oxygen concentrations than protists.

Both *O. umbonatus* and *N. truempyi* survived the PETM extinction, so they must have been resilient to the environmental changes forcing extinction of other species. *N. truempyi* was most likely epifaunal, in view of its relatively heavy carbon isotope values (26) and by analogy to its extant descendant *Nuttallides umbonifera*. The latter occurs below the lysocline and calcifies under low CO_3^{2-} and food-poor conditions (27, 28). This, in combination with paleobiogeographic evidence (29, 30), suggests that *N. truempyi* may have been adapted to low-carbonate ion bottom waters, enabling it to survive ocean acidification. *O. umbonatus* is a shallow infaunal species, as deduced from its more negative carbon isotopes values (26, 28, 31) and therefore likely adapted to the more carbonate-corrosive conditions in pore waters. At many locations, the percentage of infaunal species increased directly after the extinction (9, 29, 30), indicating preferential survival of species adapted to calcify under low carbonate saturation, thus exaptation (also called “preadaptation”) of infaunal taxa to acidification. We thus argue that under decreasing carbonate saturation, a high relative abundance of infaunal taxa cannot be seen as a proxy for decreased oxygenation and/or increased food supply, as has commonly been asserted (e.g., refs. 9, 28, 29). During the PETM, ostracods may have been less affected than benthic foraminifera because the former are less sensitive to ocean acidification (e.g., refs. 32, 33).

Both species were represented by smaller specimens during the PETM (Fig. 1), and species that became extinct may have become dwarfed just before extinction (30). Foraminifera produce smaller tests due to early reproduction (typical for opportunistic species), low oxygen conditions, or decreased carbonate saturation (34). Across the acidification intervals there were no significant differences in the number of chambers (indicative of age at reproduction) or in the proloculus size (first chamber) of *O. umbonatus* (ANOVA, $P > 0.05$) (Dataset S1), which reflects sexual (small proloculus) vs. asexual (large proloculus) reproduction. We thus found no evidence for a change in reproductive strategy or age structure, suggesting that the smaller size resulted from the addition of smaller chambers, suggesting a slower growth rate of the studied survivor species.

Our findings highlight the large gaps in our knowledge of the response of marine calcifiers in general, and foraminifers in particular, to rapid climate change. For instance, we have no information on test morphology of benthic foraminifera under different saturation states in the present oceans. The fact that *O. umbonatus* and *N. truempyi* survived the severe extinction indicates exaptation and/or resilience to PETM conditions of these taxa, both of which have very long species ranges (tens of millions of years). Molecular studies of deep-sea benthic foraminifera (including *O. umbonatus*) reveal high genetic similarity of widely separated populations (35), which may imply a high degree of plasticity within the species, which enables it to cope with varying environmental conditions.

Understanding the response of a variety of organisms and their interactions through study of the geological record of ocean acidification therefore may help us understand how organisms will respond to the combined challenges of future climate change and ocean acidification.

Methods

Measurements were performed at the TOMCAT beamline at the Swiss Light Source, Paul Scherrer Institute, Villigen, Switzerland (36). For each tomographic scan, 1,501 projections over 180° were acquired at an energy of

15 keV with UPLAPO 20× objective (numerical aperture 0.7; field view of $0.75 \times 0.75 \mu\text{m}^2$; pixel size $0.37 \times 0.37 \mu\text{m}^2$). A total of 61 specimens were scanned. The exposure time ranged between 300 and 400 ms. Projections were rearranged into corrected sinograms and reconstructed using optimized fast Fourier transform transformations and gridding procedures (37). The final data were exported as TIFF images (8-bit, 2×2 binned). Further processing to produce 3D isosurface and sample thickness was done using Avizo software. Size normalization for the penultimate chamber was done by measuring the maximum width of the foraminifera. For the volume

normalization, the volume of calcite and the overall volume of the foraminifera were calculated.

ACKNOWLEDGMENTS. This work was funded by UK National Environmental Council Grant NE/F017383/1 and Swiss Light Source Grant 20090840. This research project has been supported by the European Commission under the 7th Framework Programme: Research Infrastructures, Grant Agreement 226716. L.C.F. gratefully acknowledges the Holmes Fellowship. D.N.S. and A.R. are supported by The Royal Society in the form of University Research Fellowships and E.T. by National Science Foundation Grant OCE 0902959 and the Leverhulme Trust.

- Gattuso J-P, Hansson L (2011) *Ocean Acidification* (Oxford Univ Press, Oxford).
- Zachos JC, et al. (2005) Rapid acidification of the ocean during the Paleocene-Eocene thermal maximum. *Science* 308(5728):1611–1615.
- Hönisch B, et al. (2012) The geological record of ocean acidification. *Science* 335(6072):1058–1063.
- Haywood AM, et al. (2011) Are there pre-Quaternary geological analogues for a future greenhouse warming? *Philos Trans R Soc Lond A* 369(1938):933–956.
- McInerney FA, Wing SL (2011) The Paleocene-Eocene Thermal Maximum: A perturbation of carbon cycle, climate, and biosphere with implications for the future. *Annu Rev Earth Planet Sci* 39:489–516.
- Kennett JP, Stott LD (1991) Abrupt deep-sea warming, palaeoceanographic changes and benthic extinctions at the end of the Paleocene. *Nature* 353:225–229.
- Tripati A, Elderfield H (2005) Deep-sea temperature and circulation changes at the Paleocene-Eocene Thermal Maximum. *Science* 308(5730):1894–1898.
- Zachos JC, et al. (2003) A transient rise in tropical sea surface temperature during the Paleocene-Eocene thermal maximum. *Science* 302(5650):1551–1554.
- Thomas E (2007) *Large Ecosystem Perturbations: Causes and Consequences*, eds Monechi S, Coccioni R, Rampino MR (Geological Society of America, Boulder, CO), pp 1–23.
- Gibbs SJ, Bown PR, Sessa JA, Bralower TJ, Wilson PA (2006) Nannoplankton extinction and origination across the Paleocene-Eocene Thermal Maximum. *Science* 314(5806):1770–1773.
- Kelly DC, Bralower TJ, Zachos JC, Premoli-Silva I, Thomas E (1996) Rapid diversification of planktonic foraminifera in the tropical Pacific (ODP Site 865) during the late Paleocene thermal maximum. *Geology* 24(5):423–426.
- Gibbs SJ, Stoll HM, Bown PR, Bralower TJ (2010) Ocean acidification and surface water carbonate production across the Paleocene-Eocene thermal maximum. *Earth Planet Sci Lett* 295(3–4):583–592.
- Stap L, Lourens L, van Dijk A, Schouten S, Thomas E (2010) Coherent pattern and timing of the carbon isotope excursion and warming during Eocene Thermal Maximum 2 as recorded in planktic and benthic foraminifera. *Geochem Geophys Geosyst* 11:Q11011.
- Stap L, et al. (2010) High-resolution deep-sea carbon and oxygen isotope records of Eocene Thermal Maximum 2 and H2. *Geology* 38(7):607–610.
- Thomas E, Zachos JC (2000) Was the late Paleocene thermal maximum a unique event? *GFF* 122:169–170.
- Stap L, Sluijs A, Thomas E, Lourens L (2009) Patterns and magnitude of deep sea carbonate dissolution during Eocene Thermal Maximum 2 and H2, Walvis Ridge, southeastern Atlantic Ocean. *Paleoceanography* 24:PA1211, 10.1029/2008PA001655.
- Barker S, Elderfield H (2002) Foraminiferal calcification response to glacial-interglacial changes in atmospheric CO₂. *Science* 297(5582):833–836.
- McCarren H, Thomas E, Hasegawa T, Röhl U, Zachos JC (2008) Depth dependency of the Paleocene-Eocene carbon isotope excursion: Paired benthic and terrestrial biomarker records (Ocean Drilling Program Leg 208, Walvis Ridge). *Geochem Geophys Geosyst* 9:Q10008, 10.1029/2008GC002116.
- de Nooijer LJ, Toyofuku T, Oguri K, Nomaki H, Kitazato H (2008) Intracellular pH distribution in foraminifera determined by the fluorescent probe HPTS. *Limnol Oceanogr Methods* 6:610–618.
- Bijma J, Spero HJ, Lea DW (1999) *Use of Proxies in Paleoceanography: Examples from the South Atlantic*, eds Fischer G, Wefer G (Springer, Berlin), pp 489–512.
- Dissard D, Nehrke G, Reichart GJ, Bijma J (2010) Impact of seawater pCO₂ on calcification and Mg/Ca and Sr/Ca ratios in benthic foraminifera calcite: results from culturing experiments with *Ammonia tepida*. *Biogeosciences* 7:81–93.
- Haynert K, Schönfeld J, Riebesell U, Polovodova I (2011) Biometry and dissolution features of the benthic foraminifer *Ammonia aomoriensis* at high pCO₂. *Mar Ecol Prog Ser* 432:53–67.
- Allison N, Austin W, Paterson D, Austin H (2010) Culture studies of the benthic foraminifera *Elphidium williamsoni*: Evaluating pH, Δ[CO₃²⁻] and inter-individual effects on test Mg/Ca. *Chem Geol* 274(1–2):87–93.
- Yasuhara M, et al. (2012) Climatic forcing of Quaternary deep-sea benthic communities in the North Pacific ocean. *Paleobiology* 38(1):162–179.
- Webb AE, Leighton LR, Schellenberg SA, Landau EA, Thomas E (2009) Impact of the Paleocene-Eocene thermal maximum on deep-ocean microbenthic community structure: Using rank-abundance curves to quantify paleoecological response. *Geology* 37(9):783–786.
- Katz ME, et al. (2003) Early Cenozoic benthic foraminiferal isotopes: Species reliability and interspecies correction factors. *Paleoceanography* 18(2):1024, 10.1029/2002PA000798.
- Bremer ML, Lohmann GP (1982) Evidence for primary control of the distribution of certain Atlantic Ocean benthonic foraminifera by degree of carbonate saturation. *Deep-Sea Res A, Oceanogr Res Pap* 29(8):987–998.
- Jorissen FJ, Fontanier C, Thomas E (2007) *Proxies in Late Cenozoic Paleoceanography (Pt. 2): Biological Tracers and Biomarkers*, eds Hillaire-Marcel C, de Vernal A (Elsevier, New York), pp 263–326.
- Thomas E (1998) *Late Paleocene-Early Eocene Climatic and Biotic Events in the Marine and Terrestrial Records*, eds Aubry M-P, Lucas SG, Berggren WA (Columbia Univ Press, New York), pp 214–243.
- Winguth AME, Thomas E, Winguth C (2012) Global decline in ocean ventilation, oxygenation, and productivity during the Paleocene-Eocene Thermal Maximum: Implications for the benthic extinction. *Geology* 40(3):263–266.
- Thomas E, Shackleton NJ (1996) The Paleocene-Eocene benthic foraminiferal extinction and stable isotope anomalies. *Geological Society of London Special Publications* 101: 401–441.
- Melzner F, et al. (2009) Physiological basis for high CO₂ tolerance in marine ectothermic animals: pre-adaptation through lifestyle and ontogeny? *Biogeosciences* 6: 2313–2331.
- Payne JL, Clapham ME (2012) End-Permian mass extinction in the oceans: An ancient analog for the twenty-first century? *Annu Rev Earth Planet Sci* 40:89–111.
- Boltovskoy E, Scott DB, Medioli FS (1991) Morphological variations of benthic foraminiferal tests in response to changes in ecological parameters: A review. *J Paleontol* 65(2):175–185.
- Pawlowski J, et al. (2007) Bipolar gene flow in deep-sea benthic foraminifera. *Mol Ecol* 16(19):4089–4096.
- Stampanoni M, et al. (2006) *Developments in X-Ray Tomography V*, ed. Bonse, U (SPIE, Bellingham, WA), 101117/12679497.
- Marone F, Muench B, Stampanoni M (2010) *Developments in X-Ray Tomography VII*, ed. Stock SR (SPIE, Bellingham, WA), 10.1117/12.877483.
- Röhl U, Westerhold T, Bralower TJ, Zachos JC (2007) On the duration of the Paleocene-Eocene thermal maximum (PETM). *Geochem Geophys Geosyst* 8: Q12002, 12010.11029/12007GC001784.